

Electrospark Graphite Alloying of Steel Surfaces: Technology, Properties, and Application

V. B. Tarel'nik^{a, *}, A. V. Paustovskii^{b, **}, Yu. G. Tkachenko^{b, **}, V. S. Martsinkovskii^a,
A. V. Belous^a, E. V. Konoplyanchenko^a, and O. P. Gaponova^{c, ***}

^aSumy National Agrarian University, Sumy, 40021 Ukraine

^bFrantsevich Institute of Materials Science Problems, NAN of Ukraine, Kiev, 03680 Ukraine

^cSumy State University, Sumy, 40007 Ukraine

*e-mail: tarelnik@i.ua

**e-mail: tkachenko_yuri@ukr.net

***e-mail: gaponova@pmtkm.sumdu.edu.ua

Received January 18, 2017

Abstract—Regularities in the influence of processing time and discharge energy on the thickness, microhardness and roughness of carburized cases during electrospark graphite alloying of steel surfaces are studied and quantitative data on them are obtained. The thickness of the strengthened layer increases with gains in discharge energy and alloying time. Specimens of 40Kh, 38KhMYuA, 40KhN2MYuA, 30Kh13, Armco iron, 12Kh18N10T steels and 20 steel, as well as EGe-4 graphite are studied. The tests were carried out using the following devices: EILV-8A, EILV-9, Elitron-22A, and Elitron-52A, which provide discharge energy in the range from 0.1 to 6.8 J. Experiments show that case depth and microhardness under the same process conditions are differ significantly for various steel grades. Case depth increases with higher initial carbon contents in steel. The greater the discharge energy, the greater this difference is. Wear tests show that the method of nonabrasive ultrasonic finish processing after graphite electrospark alloying is effective, and it allows increases in the wear resistance of specimens by a factor of 7.8 for 40Kh steel and by a factor of 11.5 for 12Kh18N10T steel. Research confirms that the stage electrospark alloying of the surface of a specimen after carbonization with a graphite electrode effectively decreases roughness. Discharge energy is lowered at each stage. The stage graphite electrospark alloying of the 38KhMYuA steel case allowed decreases in the surface roughness from $R_a = 11.9\text{--}14.0\ \mu\text{m}$ to $0.8\text{--}0.9\ \mu\text{m}$. Industrial tests show that graphite electrospark alloying offers can accomplish a number of practical tasks.

Keywords: graphite, electrospark coatings, spark discharge energy, carbonization, wear-resistance, surface roughness, microhardness, alloyed steel

DOI: 10.3103/S106837551802014X

INTRODUCTION

When graphite is used as an anode in the process of electrospark alloying, allowed much room must be taken up in obtaining the desired properties of steel surfaces. The surfaces of the electrode are exposed to local action of high shockwave pressures and temperatures [1, 2]. There is an instantaneous heating of the anode, and a drop from or a solid particle of the anode material moves to the cathode. The parts that fly from the anode to the cathode are heated to high temperatures. The discharge of sparks takes place within microscopically small volumes and proceeds for 50–400 μs . Dimples and microbaths are formed on the cathode where the anode and cathode particles interact with each other and with the environment, diffusion processes are activated that lead to the formation of new phases and to changes in the structure of the

surface layer. In existing research on the use of graphite in electrospark processes, both investigation of phase changes in the surface layers of iron alloys in graphite electrospark alloying (ESA) and the improvement of this process.

It has been found [3] that in the graphite ESA of iron alloys a hardened layer is formed that combines viscous austenite and solid carbide. The high cooling rate leads to the formation of a phase composition with a metastable diagram through generating carbides and other metastable phases. Here, graphite is not liberated. With compact metal electrodes and graphite, ferrosilicon, or copper powders, in the formed layer graphite can be found, used as a dry lubricant to improve the performance of the friction coupling parts of steel, titanium, and copper alloys [4]. Investigations of the mechanism of phase formation of electrospark carbonization (EC) [5] showed that a cementite phase

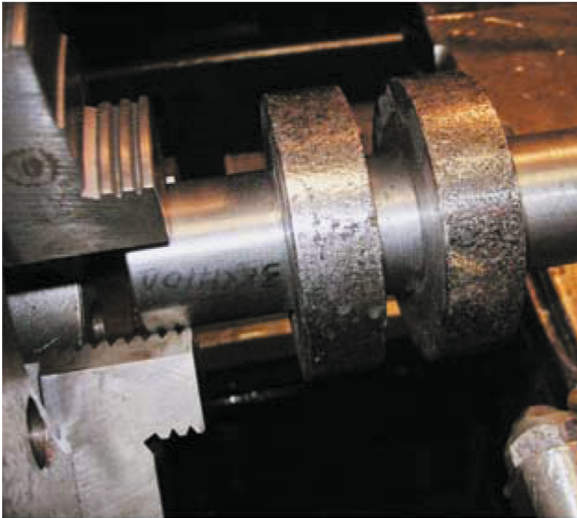


Fig. 1. Nonabrasive ultrasonic finishing processing of a steel specimen after electrospark carbonization.

(Fe_3C) is generated in the surface layer of steel samples, with the following stages: liquid phase, saturation with carbon and nitrogen ions, and then high-speed crystallization with the generation of residual austenite and iron nitride (Fe_4N). To increase their wear and corrosion resistance in a number of chemical media the copper parts were processed using ESA with aluminum electrodes and then with graphite electrodes [6].

ESA with a graphite electrode is not attended by any increase in part size to allow its comparison with kind of thermochemical treatment (carbonization) [7]. It should be noted that for conventional carbonization (heating to a temperature of 900–950°C and holding for 10 hours in the carburizing compound to produce a layer of 1 mm), one should ground much of the surface layer (its hardest part) to remove the bucklings and distortions. The desired results are not always achieved with this method.

In electrosparking, graphite is also used to decrease the roughness of surfaces that are formed through electrospark preprocessing with other electrode materials (copper, silver, nickel, and titanium) [8]. The most effective influence on surface roughness is exerted by graphite ESA where the preprocessing is carried out using electrodes made of metals that do not generate solutions with carbon or carbide.

The process of ESA of surfaces using a graphite electrode and different processes to reduce the roughness of steel samples after EC are applied when it is necessary to improve the wear resistance and operational life of the parts of equipment and instruments [9–13].

Research and practice show prospect in this area of electrospark technology. Data have been accumulated on the phase and structural transformations in surface layers of steels and various metals in graphite ESA.

Information on the influence of the structure and properties of the process conditions and machining processes of the carburized surfaces is available. However, there are little quantitative data concerning the influence of the discharge energy on the depth of carbonization, the properties and roughness of metal surfaces, or the effects of EC on the strength of the steel samples. It is necessary to improve the carburized surface processing to decrease roughness and to improve the properties.

This work has the following aims:

- study the influence of discharge energy and alloying time on case depth, microhardness, and surface roughness;

- establish the most reasonable modes of the carburized surface machining, using the method of stage graphite ESA and the method of nonabrasive ultrasonic finish processing (NUFP) to decrease the roughness and improve the properties;

- investigate the influence of EC on the wear resistance and the strength at extending the steel specimens; and

- evaluate the research results for industry.

RESEARCH TARGETS AND TECHNIQUE

To accurately obtain desired parameters of size and roughness for work surface after ESA with graphite, one must perform additional methods of processing, such as disc grinding and NUFP [14]. The latter is due to the fact that in the course of processing between the deforming element and the surface, there is periodic contact with the frequency of ultrasonic vibrations. At the moment of contact, instantaneous stresses are considerably higher than average, causing substantial plastic deformation. As in the case of other methods of surface deformation (smoothing, rolling, etc.) processing leads to decreases in surface roughness. Experiment has shown that the NUFP allows the problems of tension stresses in the layer formed by ESA to be solved, balancing them using the compression stresses which appear in the course of processing. The NUFP was carried out using a 16Ka20 screw-cutting lathe with PMS-39 magnetostriction transducer and an UZU-030 ultrasonic generator.

Specific steel specimens were used in the form of a coil consisting of two discs 50 mm in diameter and 100 mm in width connected with intermediate spindles 15 mm in diameter, possessing two technical parts with the same diameter, mounted in a holder. The surfaces of the discs were polished to $R_a = 0.5 \mu\text{m}$ before EC. The specimens were fixed in the turning lathe holder, and then automated EC and NUFP were carried out (Fig. 1).

The specimens of 40Kh, 38KhMYuA, 40KhN2MYuA, 30Kh13, Armco iron, 12Kh18T10T steels and plate specimens of 20 steel $15 \times 15 \times 6$ in size were studied. EG-4 grade graphite was used as an elec-

trode. The EC was carried out using the devices EILV-8A and EILV-9. The devices Elitron-22A and Elitron-52A, which provided discharge energy from 0.1 to 6.8 J, were used to decrease roughness when investigating the stage EC method.

The metallographic study of the microsection surface layer specimens was carried out using a Neofot-21 optical microscope. Microhardness was measured with the help of a PMT-3 microhardness tester pressing in a diamond pyramid under a load of 0.5 N.

The depth of carbonization (h) was determined using the metallographic method as a distance from the surface of the article to the center of the transition zone. As a rule, the transition zone is hypereutectoid, where the structure contains the same volumes of ferrite and perlite.

Specimen EC time was 5 min/cm². Experiments have shown that the growth in the strengthened layer depth slowed sharply after 5 minutes of EC (Fig. 2). At a discharge energy of 0.5 J, the strengthened layer is almost completely formed within a minute.

The most suitable EC time for the specimen unit area in the stage of processing to decrease roughness was determined experimentally according to the surface damaging degree (Table 1). At longer processing times the roughness changed little.

The modes of EC and the methods of surface processing are given together with the investigation results.

To approve an integration of the processes of strengthening of steel parts using EC and NUFP comparative tests were carried out on for wear resistance to substitute the processes for the production of protection sleeves of oil seals of Monel metal used in centrifugal type compressors. Wear-resistance tests were conducted using an SMC-2 friction machine with a ring-plate specimen pattern [15]. The rings were manufactured of 40Kh and 12Kh18N10T steels and Monel metal with coatings made using a conventional process. A triangular specimen of the Te15Ka6 solid alloy with a work surface roughness of $R_a = 1.6 \mu\text{m}$ was used as a counterbody. The tests were performed under conditions of limited lubrication. I20 industrial oil was used as a lubricant. Wear resistance was estimated using to the linear wear of the surface of the specimen using the method of artificial bases (GOST 16524-72). Sliding velocity was $V = 0.8 \text{ m/s}$, the load was 10 MPa, and the test time was 9 h, corresponding to a sliding distance of 26 km.

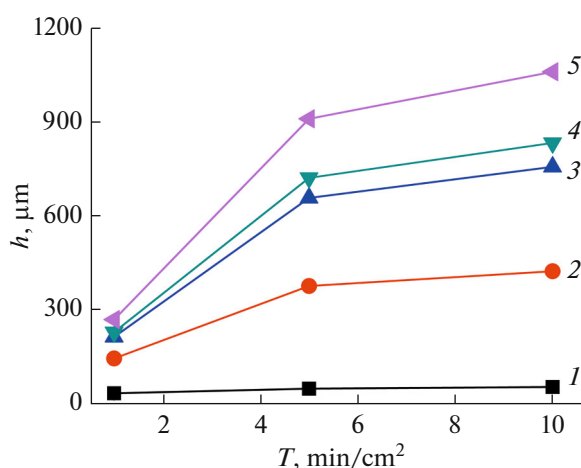


Fig. 2. Strengthened layer depth versus time of graphite alloying of 40Kh steel at a discharge energy of 0.5 (1), 1.41 (2), 2.83 (3), 3.4 (4), and 6.8 (5) J.

Surface roughness was measured at each research stage, using a profile recorder (model 201 profile meter from the Kalibr plant, modified to transfer the results to a computer using a special device).

Static tests for the expansion of specimens 10 mm in diameter and 50 mm long before and after EC were performed according to a conventional procedure (GOST 1497-84).

RESEARCH RESULTS

The efficiency of the usage of the strengthened part of the surface is related to both the parameters of the geometric surface (roughness, waviness), because most damages begin on the surface, and the properties of the boundary layer and the strengthened layer. In the course of study, the main parameters for the estimation of the quality of the surface layer after the EC were as follows: the thickness, microhardness and structure, and surface roughness of the carbonized layer. We studied the structure and hardness of the steel specimens' cores simultaneously. Our experiments showed that, with the growth in processing time and discharge energy, the carbonized layers are thicker and the basic material structure remains the same (Fig. 3).

Three characteristic zones can be distinguished in the structure of the specimens: the carbonized (white) layer, a transition zone with finely dispersed grains, and the zone of the main metal zone. As the distance

Table 1. Electrospark carbonization time as a function of discharge energy

Discharge energy, J	0.1	0.31	0.53	0.9	2.83	3.4	6.8
EC capacity, min/cm ²	2	1.0	1.0	1.0	0.5	0.5	0.5

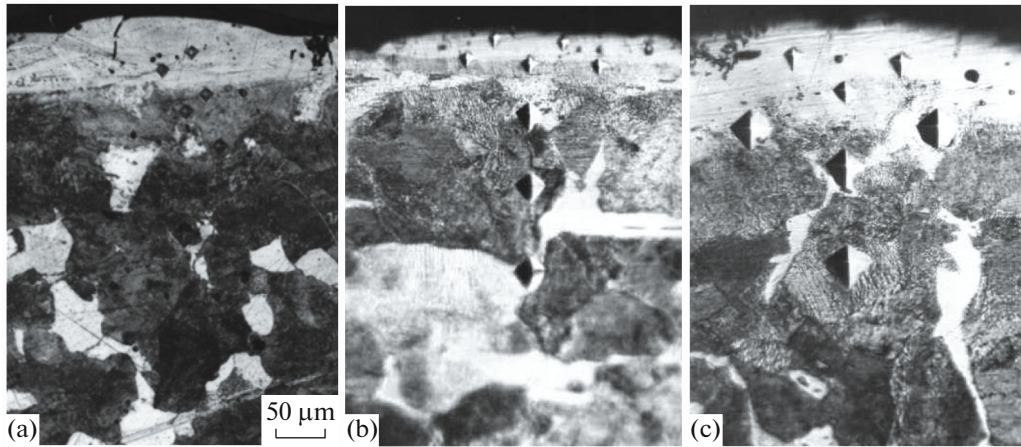


Fig. 3. Cross section view of specimens of 38KhMYuA (a) and 40Kh (b, c) steels after electrospark carbonization. Processing time was 1 min/cm²: (a) $W_p = 0.9$ J, $\times 200$. (b) $W_p = 0.60$ J, $\times 200$, and (c) $W_p = 2.60$ J, $\times 250$.

to the surface decreases the microhardness in the boundary layer grows. Microhardness on the surface is 1350 and 760 HV for 38KhMYuA and 40KhN2MYuA steels, respectively (Fig. 4). As it deepens, the microhardness drops and smoothly passes into a basis hardness of 225 and 250 HV, respectively. Decreases in the hardness on the surface of the carbonized specimens are associated with the structure of the strengthened layer, the presence of a thin troostite (dispersed mixture of ferrite iron carbide) band or network on the surface. The troostite band is 50–60 μm thick. As a rule, after the NUFPP, this band is absent. Test showed that at the EC of 20 steel there is no troostite band.

In the carbonization of steel surfaces using ESA, the thickness of the strengthened layer grows with increases in discharge energy and alloying time. Sur-

face roughness grows as well (Fig. 5). Peak microhardness on the 38KhMYuA steel surface is variable, from 900 to 1010 MPa.

The results of the examination of the general thickness of higher hardness layer, peak microhardness on the surface, and the roughness after EC, NUFPP, and polishing of 40Kh and 12Kh18N10T steels are presented in Table 2.

The investigations showed that the depth of the carbonized layer and its microhardness under the same process conditions vary greatly for various steel grades. We conducted a set of experiments with steels of various compositions. Figure 6 presents the measurements for the depth of the strengthened layer at EC at 1 and 5 min/cm² of the substrates of Armco iron

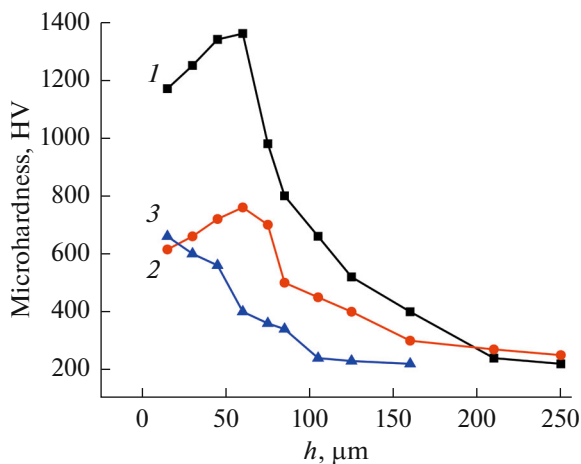


Fig. 4. Distribution of HV microhardness in carbonized layer of 38KhMYuA (1) and 40KhN2MYuA (2) steels after electrospark carbonization ($W_p = 0.9$ J, 5 min/cm²) and 40Kh steel after stage carbonization ($W_p = 2.83$ and 0.9 J, 5 and 2 min/cm², respectively) and nonabrasive ultrasonic finishing polishing (3).

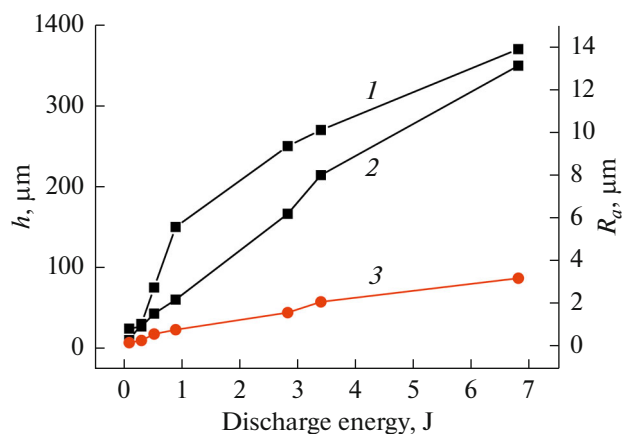


Fig. 5. Dependence of carbonized layer thickness h (1) and the surface roughness R_a on discharge energy after electrospark carbonization (2) and after electrospark carbonization and nonabrasive ultrasonic finishing polishing (3) of 38KhMYuA.

Table 2. Layer depth, surface microhardness, and roughness of the 40Kh and 12Kh18N10T surfaces of the steel sample after electrospark carbonization using nonabrasive ultrasonic finishing of metals and polishing

Discharge energy, J	Sample processing method	After-treatment layer depth, m		Microhardness, HV		Roughness R_a , m,	
		40Kh	12Kh18N10T	40Kh	12Kh18N10T	40Kh	12Kh18N10T
0.6	EC + NUFM	50	50	980	880	0.2	0.2
	EC + NUFP + P	40	48	920	841	0.6	0.6
	EC + P	10	18	780	723	0.6	0.6
	EC	50	48	987	1013	0.8–0.9	0.9–1.0
2.83	EC + NUFP	657	210	920	970	0.8	0.8
	EC + NUFP + P	635	195	895	950	0.8	0.8
	EC + P	580	130	770	790	0.8	0.8
	EC	658	200	1000	974	5.6–6.5	5.8–6.7
6.8	EC + NUFP	908	244	854	985	0.8	0.8
	EC + NUFP + P	895	220	840	875	0.8	0.8
	EC + P	856	110	824	670	0.8	0.8
	EC	910	250	1050	1100	11.9–14.1	10.0–14.5

and certain steels for different values of discharge energy.

Experiments showed a distinct dependence: the thicker the carbonized layer thickness is, the higher the carbon content in the steel. Carbonization depths of 40Kh and 30Kh13 steels with an average content of carbon in the initial state are close to 0.3–0.4%, which is substantially higher than that of Armco iron and 12Kh18N10T steel containing up to 0.12% carbon. The greater the discharge energy the higher the difference. For the EC of 40Kh and 12Kh18N10T steels at

5 min/cm² with a discharge energy of 6.8 J, the difference in the strengthened layer thicknesses reaches 660 μm .

STAGE EC METHOD

Although the NUFP of steel surfaces after ESA with a graphite electrode substantially decreases their roughness, for many machine parts this is insufficient. Polishing after EC is found to be impossible, as in this case not less than 50–100 μm of the surface layer with

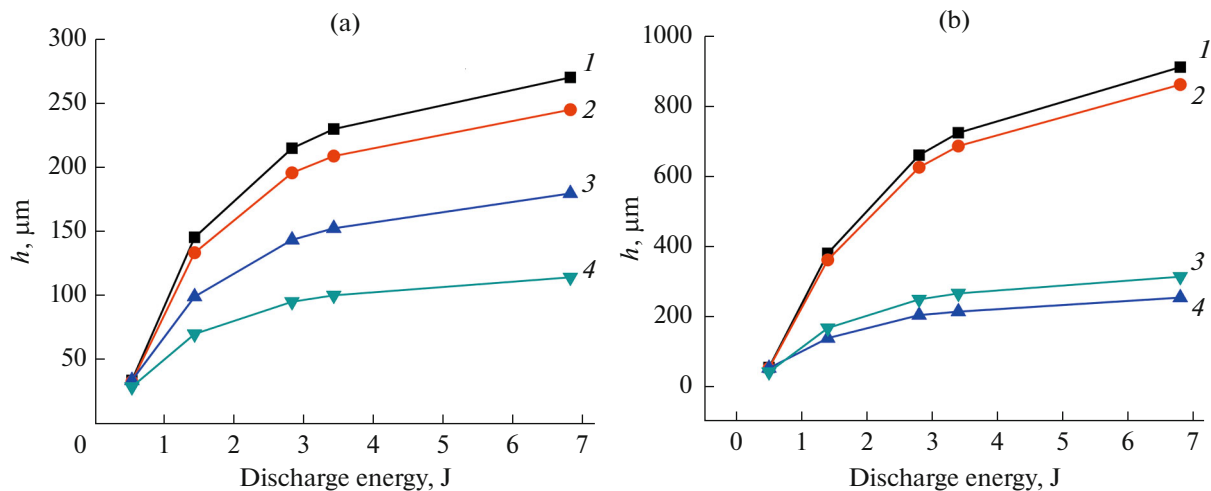


Fig. 6. Carbonized layer thickness h versus discharge energy after EC of surface during 1 (a) and 5 (b) min/cm² of 40Kh (1), 30Kh13 (2), Armco iron steels (3), and 12Kh18N10T steel (4).

Table 3. Decrease in surface roughness of steel specimens after electrospark carbonization

Steel grade	Discharge energy, W_p , J	Roughness, R_a , μm Productivity, T , min/cm^2						
		after EC	discharge energy, W_p , J					
			0.1	0.31	0.53	0.9	2.83	3.4
38KhMYuA	0.1	0.8–0.9						
	0.31	0.9–1.0	$\frac{0.8-0.9}{2}$					
	0.53	1.4–1.7	$\frac{0.8-0.9}{2}$	$\frac{0.9-1.0}{1}$				
	0.9	1.7–2.1	$\frac{0.9-1.0}{2}$	$\frac{1.0-1.1}{1}$	$\frac{1.4-1.7}{1}$			
	2.83	5.7–6.9	$\frac{1.1-1.2}{14}$	$\frac{1.2-1.3}{6}$	$\frac{1.6-1.9}{3}$	$\frac{1.7-2.2}{2}$		
	3.4	8.3–8.9	$\frac{1.3-1.6}{18}$	$\frac{1.4-1.7}{7}$	$\frac{2.0-2.3}{4}$	$\frac{2.3-2.7}{3}$	$\frac{5.7-6.7}{0.5}$	
	6.8	11.9–14.0	$\frac{1.6-1.9}{25}$	$\frac{1.8-2.1}{13}$	$\frac{2.4-2.6}{8}$	$\frac{2.6-3.1}{5}$	$\frac{6.3-6.9}{0.5}$	$\frac{8.5-9.0}{0.5}$
40KhN2MYuA	2.83	5.7–6.7	$\frac{1.0-1.1}{14}$	$\frac{1.2-1.3}{6}$	$\frac{1.5-1.8}{3}$	$\frac{1.7-2.1}{2}$		
12Kh18N10T	2.83	2.9–3.7	$\frac{0.8-0.9}{14}$	$\frac{1.0-1.2}{6}$	$\frac{1.5-1.8}{3}$	$\frac{1.7-2.0}{2}$		

the highest hardness is removed. Soft graphite alloying is reported to be a sufficient finishing to decrease the roughness of the electrospark coating. Smoothing is due both to heating and softening the crests under the action of the hot electrode and slopping the cathode metal as well as the destruction of the projecting parts of the surface at the places of impulse application [8, 16]. The experiment showed that soft alloying with graphite does not always sufficiently decrease the surface roughness. We used the ESA process of the surface specimen after carbonization with the same graphite electrode as with the carbonization in stages, and the spark discharge energy was reduced at each next stage [9, 10]. At each next stage ESA was performed the with a graphite electrode with such a level of discharge energy that a surface was formed with a roughness 2–3 times lower than in the previous stage. The alloying time experimentally determined varied with the value of the discharge energy from 0.5 to 2 min/cm^2 (Table 1). The increase in the alloying time aids in the reduction in the surface roughness value.

Table 3 presents the results of the stage reduction in the roughness value of the specimen after EC with different discharge energy. Thus, for example, after EC is conducted on the 38KhMYuA steel, with a discharge energy of 2.83 J, the surface roughness is $R_a = 5.7\text{--}6.9 \mu\text{m}$. After ESA with a graphite electrode with $T =$

2 min/cm^2 and using the mode with a discharge energy of 0.9 J, the surface roughness is $R_a = 1.7\text{--}2.2 \mu\text{m}$. In the following stage alloying one can reach $R_a = 1.1\text{--}1.2 \mu\text{m}$.

The results of the stage reduction in the roughness of 40KhN2MYuA and 12Kh18N10T steels after EC with a discharge power of $W_p = 2.83 \text{ J}$ are presented in Table 3 for comparison.

With the aim of minimizing the surface roughness of, say, 38KhMYuA steel after EC with a discharge energy of 6.8 J to $R_a = 11.9\text{--}14.0 \mu\text{m}$, we must do the following:

—carry out the graphite ESA at $W_p = 2.83 \text{ J}$ in the first stage, i.e., with discharge energy bringing the roughness value (from 11.9–14.0 to 6.3–6.9 μm) down by a half: the ESA time was 0.5 min/cm^2 ;

—carry out graphite ESA at $W_p = 0.9 \text{ J}$ in the second stage, i.e., with discharge energy providing a decrease in the roughness value by a factor of nearly 3 (from 6.3–6.9 to 1.7–2.1 μm): the ESA time was 2 min/cm^2 ;

—carry out graphite ESA at $W_p = 0.1 \text{ J}$ in the third stage, i.e., with discharge energy providing nearly halving the roughness value (from 1.7–2.1 to 0.8–0.9 μm): the ESA time was 2 min/cm^2 .

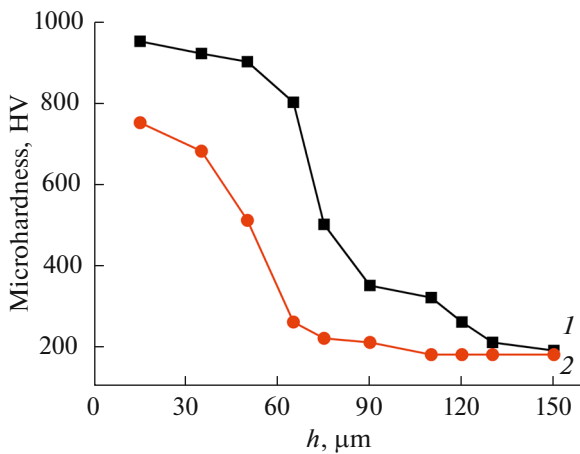


Fig. 7. Distribution of HV microhardness through the depth of the carbonized layer of 20 steel after EC at $W_p = 2.83$ J (1) and after stage EC at $W_p = 2.83, 0.9$, and 0.1 J (2).

The stage graphite ESA of the carbonized layer of 38KhMYuA steel allowed a reduction in surface roughness from $R_a = 11.9$ – 14.0 μm to 0.8 – 0.9 μm .

It should be noted that single-stage ESAs with a graphite electrode decrease surface roughness after EC in any mode make it impossible to obtain similar results.

Analyzing the distribution of microhardness in the 20 steel specimens after EC at $W_p = 2.83$ J and stage EC at $W_p = 2.83, 0.9$, and 0.1 J (Fig. 7), it can be seen that in both cases, the peak microhardness of the strengthened layer is observed to be closer to the surface. For the first specimen it is 920–950 HV at a distribution depth up to 60 μm , and for the second specimen it is 690–720 HV at a depth of 30 μm . As depth increases for both specimens, the value for microhardness smoothly decreases, and at a depth of 130 and 100 μm it corresponds to a substrate microhardness of 180 HV. The decrease in the thickness of the strengthened layer and microhardness for the specimen with a stage EC can be explained by the effect of the shock action of the heated high-temperature graphite elec-

trode and the modest erosion of the substrate. It has been shown earlier [17] that a mechanical shock action on the carbonized layer causes carbide grinding and carbon redistribution in a surface layer that is 30–40 μm in thickness.

Thus, the stage EC of the 20 steel results in the decrease of the surface layer roughness from $R_a = 4.79$ to $R_a = 1.10$ μm and from $R_a = 13.62$ to $R_a = 3.14$ μm , the reduction in microhardness in the “white” layer from 920–950 HV to 690–720 HV, and the drop in the overall depth of the higher hardness zone of the surface layer, from 130 to 100 μm .

INFLUENCE OF EC AND NUFP ON STRENGTH

The appropriateness of the application to protective strengthening coatings is to a great extent determined by the value, sign, and character of the distributions of residual-process stresses within the layers of the substrate–coating system. Coating that is independent of the production method influences the mechanical properties of the material [18]. The reliability of the protection and the strengthening of articles in service, and the wear resistance of the coated construction materials largely determine the static and cyclic strength of the coated articles. In this context, the investigation of the EC influence on the strength under tension, ultimate resistance, relative extension and reduction of steel specimens is topical. The data are presented in Table 4. It is seen that the EC strengthening of the specimens results in a growth of the ultimate resistance at the extension by a factor of 1.1 and of the yield stress for the 40Kh and the 12Kh18N10T steel specimens by a factor of 1.04 by a factor of 1.06, respectively. The additional application of NUFP increases the ultimate resistance at the extension of the materials under tests by a factor of 1.22 for the 40Kh specimens and of 1.7 for the 12Kh18N10T steel specimens.

The graphite electrospark processing of steel surfaces result in the appearance of thermal stresses to the coating–substrate system. The quantity and sign of the

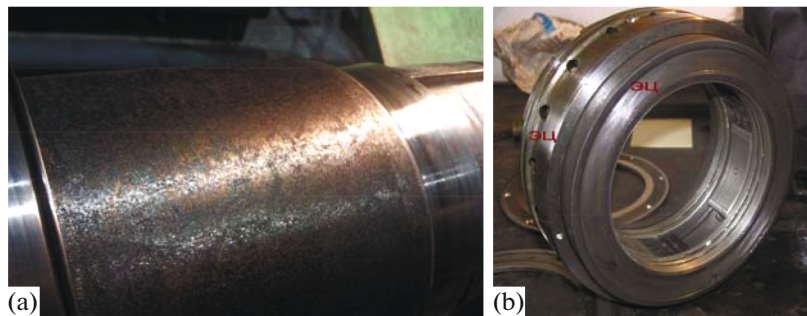


Fig. 8. The appearance of the seal unit protective sleeve after the EC (a) and the centrifugal compressor floating seal ring, which shows the locations of the EC (b).

Table 4. Expansion strength, yield stress, relative extension and reduction of the 40Kh and 12Kh18N10T steels after electrospark coating

Discharge energy, J	Yield stress, MPa		Ultimate resistance at extension, MPa		Relative extension, %		Relative reduction, %	
	EC	EC + NUFP	EC	EC + NUFP	EC	EC + NUFP	EC	EC + NUFP
40Kh steel								
–	315	315	570	570	17	17	38	38
0.6	327	375	627	695	16	18	37	36
2.83	319	380	615	690	15	18	36	35
3.4	320	378	605	685	15	17	36	36
12Kh18N10T steel								
–	196	196	510	510	40	40	55	55
0.6	208	264	530	867	39	28	54	45
2.83	207	270	526	860	37	27	55	43
3.4	207	255	525	858	37	30	53	44

stresses depend on the relation between the coefficients of the thermal expansion of the phases forming the coating and the steel, as well as the temperature ranges of the process. The data reflect the influence of residual process stresses that act on a surface layers and are formed in the course of the EC process, on the variation in the characteristics of the static strength of the construction materials. The values of the strength presented at the expansion indicate that the quantity and sign of the stresses in the carbonized layer favors growth in the strength of the steel specimen after EC.

APPLICATION OF RESEARCH RESULTS

To gain approval of the process of the graphite carbonization of steel parts using the electrospark method and the subsequent application of NUFP, comparison tests were carried out on wear resistance, with of aim of substituting the technological process for production of oil-seal protection sleeves that are used in centrifugal compressors. Monel metal (nickel-based alloy containing 27–38% copper) is traditionally used in floating seals in compressors as a closing sleeve substrate material. This alloy possesses a good corrosion resistance, a sufficiently high ultimate resistance, and good plastic properties at the hot and cold state. To increase the lifetime of the sleeves, the work surface is coated with the Hastelloy corrosion-resistant and wear-resistant nickel alloy, containing molybdenum, chrome, iron, carbon, and some alloying additives using plasma spraying and vacuum welding deposition.

The wear tests (Table 5) showed that the use EC and NUFP for graphite is effective and allows an

increase in the specimen wear resistance over the unhardened specimens of a factor of 7.8 for the 40Kh steel and of 11.5 for the 12Kh18N10T steel. Compared with the coating with Hastelloy alloy on Monel metal, the wear resistance of the specimens of 40Kh and 12Kh18N10T steels increased using EC + NUFP by factor of 1.2 and 1.1, respectively. The steel protective sleeves of the seals in the compressors have a practical use in the substitute sleeves of Monel metal.

A number of processes to strengthen compressor parts have been elaborated at the TRIZ (Partnership for Realization of Engineering Tasks, Sumy, Ukraine) factory. Two-thirds of all compressor failures of occur due to the abnormal performance of seals. Therefore, a seal assembly is one of the most important units ensuring the tightness of the compressor assembly and its reliable, safe, and trouble-free operation. The work surface of the parts of this unit must be produced of a hard, wear-resistant material, and its substrate must be sufficiently plastic to allow it to pass on a shaft and respond to the demands of endurance strength. After the heat-treated 38Kh2MYuA steel sleeve is arranged on the shaft, carbonization is performed using the electrospark method with NUFP (Fig. 8a). The surfaces of the contact ends of the sealing floating rings (Fig. 8b) and the counterparts of the casing and cover plates are similarly strengthened. The EC process for the end surfaces of the rings of the floating seals and protective sleeves was carried out using an Elitron-22A device at a discharge energy of 0.5 J. The depth of the strengthened layer reached 30–50 μm , and the micro-

Table 5. Wear of the specimens of 40Kh and 12Kh18N10T steels and the Hastelloy alloy coating on Monel metal

Process name	Linear wear of specimens, μm		
	40Kh	12Kh18N10T	Hastelloy alloy coating on Monel metal
Without strengthening	30.98	50.35	4.8
	30.89	49.78	
	31.07	50.02	
EC + NUFP	4.41	4.51	
	3.98	4.45	
	4.12	4.34	
EC + NUFP + P	4.39	4.71	
	4.18	4.69	
	4.21	4.73	
EC + P	9.51	10.02	
	9.48	10.10	
	9.56	10.08	

hardness was 900–1110 HV. Contact surfaces were alloyed with silver at a discharge energy of 0.05 J to reduce roughness and friction.

The application of the methods of EC and NUFP makes it possible to produce a high-quality strengthened surface whose parameters are achieved at lower (by a factor of 5–10) expenditure than with the help of materials and processes previously used. The EC method can be conducted without complete disassembly; parts of any size can be strengthened.

CONCLUSIONS

(1) Regularities were found in the influence of processing time and discharge energy at the graphite ESA of steel surfaces on the thickness, microhardness, and roughness of the carbonized layers and quantitative data was obtained as well. The thickness of the strengthened layer grows with the increase in discharge energy, and alloying time reaches 0.9 mm at a microhardness of 1100 HV for the 40Kh steel.

(2) The depth of the carbonized layer and its microhardness in the same process modes were shown to be greatly different for various steels grades. The depth of EC is greater where carbon contents are greater in the initial-state steel. The greater the discharge energy is, the greater this difference.

(3) Our investigation confirmed that the stage ESA with a graphite electrode of the specimen surface after carbonization efficiently decreases roughness. At each next stage, the discharge energy of the electrospark was reduced. The stage graphite ESA of the 38KhMYuA steel carbonized layer allows a decrease in the surface

roughness from a value of $R_a = 11.9\text{--}14.0 \mu\text{m}$ up to $0.8\text{--}0.9 \mu\text{m}$.

(4) The industrial evaluation of the research results showed that the graphite ESA allows the formation of surface layers on the steel part with greater hardness and wear resistance without any change in the initial size of the part. The received strength values of indicate that the value and sign of stresses in the carbonized layer improves the strength of steel specimen after EC. It makes possible to conduct a number of practical tasks that would improve the performance of the compressor parts.

REFERENCES

1. Lazarenko, B.R. and Lazarenko, N.I., *Elektroiskrovyi sposob izmeneniya iskhodnykh metallicheskikh poverkhnosti* (Electrospark Method of Transformation of Initial Properties of Metal Surfaces), Moscow: Akad. Nauk SSSR, 1958.
2. Verkhoturov, A.D., *Elektrofiz. Elektrokhim. Metody Obrab.*, 1983, no. 1, pp. 3–5.
3. Mikhailiuk, A.I., Gitlevich, A.E., Ivanov, A.I., Fomicheva, E.I., et al., *Elektron. Obrab. Mater.*, 1986, no. 4, pp. 23–27.
4. Mikhailiuk, A.I. and Gitlevich, A.E., *Surf. Eng. Appl. Electrochem.*, 2010, vol. 46, no. 5, pp. 424–430.
5. Ershov, V.M., *Sb. Nauch. Tr. Donbass. Gos. Tekh. Univ.*, 2011, no. 31, pp. 219–225.
6. Mikhailiuk, A.I., Revenko, V.G., and Natarov, N.N., *Fiz. Khim. Obrab. Mater.*, 1993, no. 1, pp. 101–106.
7. Gitlevich, A.E., Mikhailov, V.V., Parkanskii, N.Ya., and Revutskii, V.M., *Elektroiskrovoe legirovanie metallicheskikh poverkhnosti* (Electrospark Alloying of Metal Surfaces), Chisinau: Shtiintsa, 1985.

8. Mikhailyuk, A.I., *Elektron. Obrab. Mater.*, 2003, vol. 39, no. 3, pp. 21–23.
9. Martsinkovskii, V.S., Tarel'nik, V.B., and Bratushchak, M.P., RF Patent 2468899, *Byull. Izobret.*, 2012, no. 34.
10. Martsinkovskii, V.S., Tarel'nik, V.B., and Bratushchak, M.P., UA Patent 101715, *Byull. Izobret.*, 2013, no. 8.
11. Martsinkovskii, V.S. and Tarel'nik, V.B., *Metalloobrabotka*, 2011, no. 6, pp. 116–119.
12. Fanshmidt, E.M., Astafev, G.I., and Shevchenko, O.I., *Kuznechno-Shtampovochnoe Proizvod.—Obrab. Mater. Davleniem*, 2011, no. 4, pp. 26–31.
13. Mikhailyuk, A.I., *Met. Sci. Heat Treat.*, 2000, vol. 42, no. 7, pp. 279–282.
14. Kholopov, Yu.V., Zinchenko, A.G., and Savinykh, A.A., *Bezabrazivnaya ul'trazvukovaya finishnaya obrabotka metallov* (Nonabrasive Ultrasonic Metal Finishing), Leningrad: Leningr. Dom Nauchno-Tekh. Propagandy, 1988.
15. Kuksenova, L.I., Lapteva, V.G., Kolmakov, A.G., and Rybakova, L.M., *Metody ispytaniia na trenie i iznos* (Testing Methods for Friction and Wear), Moscow: Internet Inzhiniring, 2001.
16. Lazarenko, N.I., *Elektroiskrovoe legirovanie metallicheskikh poverkhnostei* (Electrospark Alloying of Metal Surfaces), Moscow: Mashinostroenie, 1976.
17. Sizova, O.V. and Kolubaev, E.A., *Russ. Phys. J.*, 2003, vol. 46, no. 2, pp. 133–137.
18. Izvolenskii, E.V., Krasnov, A.N., Matveev, N.V., Miloserdov, I.V., and Oreshchenkov, Yu.V., *Strength Mater.*, 1984, vol. 16, no. 10, pp. 1387–1390.

Translated by M. Myshkina